Performance Analysis of LDPC coded Outdoor Long-Distance Imaging MIMO System

Daiki ISHIKAWA
Dept. of Information and Communication Engineering
Nagoya University
Furo-cho, Chikusa-ku, Nagoya 464-8603, Japan
dishikaw@katayama.nuee.nagoya-u.ac.jp

Chedlia BEN NAILA, Hiraku OKADA
and Masaaki KATAYAMA
Institute of Materials and Systems for Sustainability
Nagoya University
Furo-cho, Chikusa-ku, Nagoya 464-8603, Japan
0000-0002-0556-2745, 0000-0003-2276-6421,
0000-0002-7612-390X

***Abstract*—In this work, the performance of light-emitting diode-based (LED-based) imaging Multiple Input Multiple Output (MIMO) system for long-distance outdoor transmission is evaluated, and based on the results, a proposal for improving the performances is presented. We first conducted outdoor communication experiments, and error-free transmission of 200 Mbps over 100 m was achieved without using Forward Error Correction or other error control schemes. Nonetheless, communication errors occurred at distances shorter than 100 m. Furthermore, the bit error rate (BER) differed for each beam from each transmitting LED. Therefore, we introduced Low-density Parity-check (LDPC) codes along with a decoding method that takes into account the BER of each signal beam. The effectiveness of this decoding method is predicated on the time-invariance of the BER, which we have separately confirmed through experimental data. We assume that encoded bit errors for each signal beam would follow the BER observed in our non-encoded communication experiments. Under this assumption, we assessed various LDPC codes with different code lengths and coding rates. Our results demonstrated an improvement in BER performance.**

***Index Terms*—Imaging receiver, optical wireless communication, OWC, optical MIMO, LDPC, outdoor communication**

I. Introduction

Optical wireless communication (OWC) is effective in large industrial environments, such as factories. OWC systems use light instead of radio waves. They are not affected by other equipment and are spatially restricted, making them superior in terms of security and ease of use in industrial environments [1].

Alhough the use of light-emitting diode-based (LED-based) OWC systems, which are safe for the eyes, is desirable, poor light directivity compared to lasers makes high-speed communication over long distances difficult. Thus the optical wireless Multiple Input Multiple Output (MIMO) technology [2] was used to increase communication speed. When using this method, the bit error rate (BER) worsens as the transmission distance increases, due to the impact of the mutual interference between the optical signals of the multiple LEDs [3]. To tackle this problem, we apply the imaging MIMO system [4] where the signal beams emitted from each LED are collected through a single optical system and projected/imaged onto a PD array, such as a camera lens and film. This enables us to increase the received signal strength by collecting light using a large-aperture telephoto lens and obtaining a channel matrix close to a diagonal matrix. Using this imaging MIMO system, our group achieved the communication at 100 Mbps over 50 m [5] and at 200 Mbps over 65 m [6] [7]. All these examples, however, are results given in an indoor stationary environment, and the performance of imaging MIMO systems in an outdoor environment is unknown.

In this work, we investigated the performance of an LED-based optical imaging MIMO system for outdoor communication for the first time, and based on the results, a proposal for improving the performances is presented. In an outdoor communication experiment, error-free transmission at a 200 Mbps data rate over a distance of 100 m is successfully achieved without error control scheme. At some distances, however, the imperfect adjustment of optical components causes variations in BER for each signal beams, degrading communication performance. Since the optical components are physically fixed, BER for each signal beam is considered time-invariant, and we confirmed this from actual experimental data.

Error correction using Low-density Parity-check (LDPC) codes [8] is a method for improving the performance of long-distance optical MIMO systems. LDPC codes are defined by a sparse inspection matrix, which allows error correction with relatively few operations and high coding rates. In [9] and [10], the authors show enhanced communication reliability in Gamma-Gamma MIMO-FSO systems. LDPC codes in optical MIMO systems has been studied for common random errors in each symbol, however there are few examples considering time-invariant and significantly different BER for each signal.

Therefore, we propose applying LDPC codes, which use the likelihood of each symbol during decoding, for encoding information on the transmitter side to long-distance imaging MIMO systems. On the receiver side, each signal is weighted by incorporating its BER into the likelihood of the corresponding received symbol, and the received word is then decoded. Simulation results showed that low BER was achieved by coding. Considering error-free transmission at 100 m, longer-distance communication should be possible using encoding in combination.

Joint Research with Chubu Electric Power Company and IMaS of Nagoya Univ.

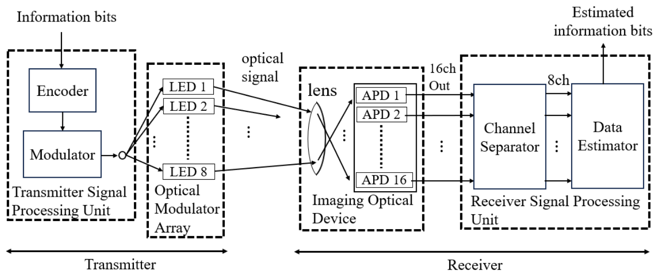

Fig. 1. Block diagram of the system

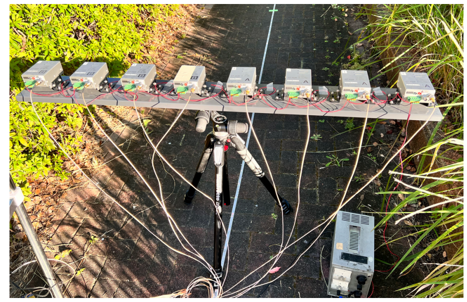

Fig. 2. Optical modulator array

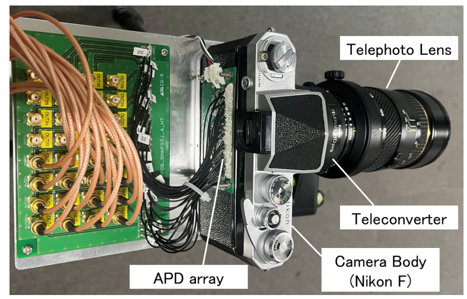

Fig. 3. Imaging optical device

TABLE I
SPECIFICATIONS OF THE EXPERIMENTAL APPARATUS

Optical element	
Wave length	820 nm (IR)
Half-value angle	1°
Imaging Optical Device	
Lens	Kenko Tokina AT-X 840AFii (focal length 80-400mmF-number 4.5-32)
IR passing filter	Kenko Tokina PRO1D R72
Teleconverter	Kenko Tokina HD pro 2X DGX (magnification 2, exposure multiple 4)

II. SYSTEM CONFIGURATION

This section provides a brief description of the experimental setup. The detailed configurations of both transmitter and receiver have already been described in our previous work [7]. Fig. 1 shows the overview of the system, and Table I outlines the specifications.

A. Transmitter

The transmitter consists of a transmitting signal processing unit and an optical modulator array with eight optical modulators, as shown in Fig. 2.

1) Transmitting Signal Processing Unit: The incoming data stream is first divided into eight streams corresponding to the eight optical modulators. The eight data streams are transmitted in a frame format that consists of a preamble for bit synchronization, a pilot for channel matrix estimation, and a payload for data transmission. Each data stream in the frame format is then encoded using Manchester coding before being passed to its corresponding optical modulator.

2) Optical Modulator Array: In the optical modulator, the input bipolar signal is converted to a nonnegative signal, which is then applied to an LED to be transmitted as an optical signal beam.

B. Receiver

The receiver comprises of an imaging optical device that optically separates the received optical signal beams into a multichannel electrical signal and a receiving signal processing unit.

1) Imaging Optical Device: As shown in Fig. 3, the imaging optical device is a modified version of a traditional film camera where the film is replaced by a linear avalanche photodiode (APD) array of 16 elements. It should noted that the focal length of the telephoto lens was appropriately set at every distance and an infrared filter was employed to eliminate unnecessary background light. Furthermore, given the telephoto lens specifications, a teleconverter was employed for distances from 70 - 100 m.

2) Receiving Signal Processing Unit: The signals from the imaging receiver's APDs are converted from analog to digital using an analog-to-digital converters (ADCs). Digital signal processing is applied to the ADC outputs offline for symbol and frame synchronization, channel matrix estimation, and data estimation.

3) Data Estimation: We use a hard decision decoder. The transmitted data are estimated based on the estimated channel matrix. Since the number of APDs exceeds the number of optical signal beams from the LEDs, the receiver selects the APD with the best performance for each beam emitting LED to estimate the data. For the m-th LED, the receiver selects the corresponding n_m-th APD, as follows

$$n_m = \arg\max_{n} \hat{h}_{n,m} \tag{1}$$

where $\hat{h}_{n,m}$ corresponds to the n-th row and m-th column element of the estimated channel matrix. Henceforth, this estimation method is referred to as "direct detection" (DD).

III. OUTDOOR EXPERIMENTS

We conducted outdoor transmission tests at Higashiyama Campus of Nagoya University. The test site is shown in Fig 4. Table II outlines the main parameters used in the experiments, whereas the conditions at each test is summarized in Table III.

Fig. 5 shows the total average BER of the received signals at different distances. An error-free transmission was achieved at

TABLE II
EXPERIMENTAL PARAMETERS

Data rate		25×8 Mbps
Peak-to-peak voltage of transmitted signal	V_{pp}	1 V
Number of optical modulators	M	8
Distance between optical modulators	D	17.5 cm
Receiver focus distance		Infinity
Aperture (F-number)		4.5
Number of APDs in the receiver	N	16
Distance between APDs	d	0.5 mm
Sampling rate		10 sample/symbol
Number of recorded frames		37 or 38
Number of recorded samples		1M×16 samples

TABLE III
EXPERIMENTt CONDITIONS

Date	Distance	Focal length	Weather	Illuminance	Time	Temparature
2022/04/20	50m	306mm	Sunny	27500lux	15:37	23.5 ℃
	60m	367mm	Sunny	24200lux	16:15	23.3 ℃
2021/12/21	70m	427mm	Sunny	20000lux	11:37	9.9 ℃
	80m	488mm	Sunny	2850lux	14:00	12.5 ℃
2022/01/24	90m	549mm	Sunny	1340lux	16:19	11.9 ℃
2022/05/19	100m	612mm	Sunny	39100lux	10:45	24.3 ℃

a distance of 100 m. Fig. 6 shows the BER of each signal at a distance of 90 m when ZF and DD techniques are considered. As can be seen, the estimation of the transmitted data is possible without any use of detection technique such as ZF. In fact, the imaging MIMO receiver has a high spatial resolution. However, the BER performance varies significantly with the transmission distance. For instance, a BER as high as 6×10^{-2} is obtained at 90 m whereas an error-free transmission can be achieved at 100 m.

Table IV shows the received signal power for all sixteen APDs' outputs at a distance of 90 m. A significant variation is evident among the received power levels of different LEDs. The emitted beams from some LEDs could not be correctly received on any of the sixteen APDs. Based on the obtained results, LEDs 1, 2, and 8 were not correctly detected by the APDs, leading to the poor performance of the total BER. Considering error-free at 100 m, imaging MIMO is capable of long-distance communication beyond 100 m. However, the imperfect adjustment of optical components is considered as the main issue rather than the attenuation at longer distances. Although the adjustment was successful at some distances and error-free is achieved, it is challenging to consistently achieve the best performance using actual equipment.

IV. INTRODUCTION OF LDPC CODING

A. Characteristic of Binary Subchannels

We label the binary channel associated with the m-th LED and n_m-th PD pair as "the m-th Binary Subchannel". As indicated in Section III, the variation in the performance of each subchannel was due to imperfect adjustment of the transmitter/receiver orientation as well as focal length. Owing to this situation, these subchannels can be assumed as time-invariant binary symmetric channels (BSC), as demonstrated by the outdoor experimental results shown in Fig. 7 at a distance of 90 m. This figure divides the total observation time of 4×10^{-3} seconds into 37 segments and shows the bit error rate of data from each LED in each segment. From this figure, it is evident that, with a few exceptions, the bit error rates are nearly uniform across the segments.

The binary symmetry of each subchannel was then confirmed using the same data, as shown in Table V. Here, P_{e+} and P_{e-} are the probabilities of flipping from $+1$ to -1 and from -1 to $+1$, respectively.

B. Coding and Decoding

Considering that subchannels are time-invariant, we applied the error-correcting coding, LDPC codes. We adopted Maximum a posteriori (MAP) estimation, using the sum-product algorithm commonly used in decoding LDPC codes, and per-symbol likelihood metrics. To carry out weighted decoding, we used BER of each signal beam as the likelihood

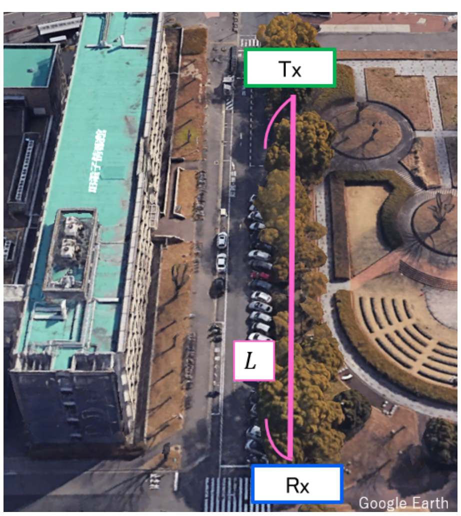

Fig. 4. Test site location

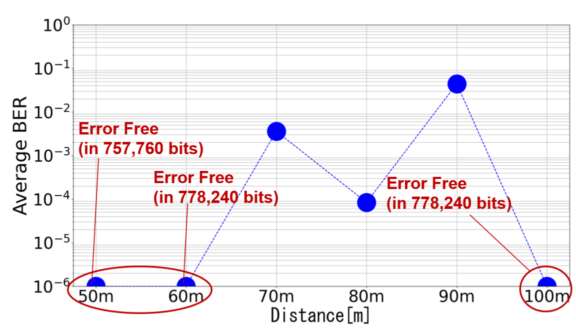

Fig. 5. Total bit error rate performance at different distances (Direct Detection)

TABLE IV
RECEIVED SIGNAL POWER AT EACH APD OUTPUT

APD n	APD1	APD3	APD5	APD7	APD9	APD11	APD13	APD15
received power (dBm)	-13.4	-18.3	-1.06	-2.49	-3.42	-4.57	-2.93	-10.24

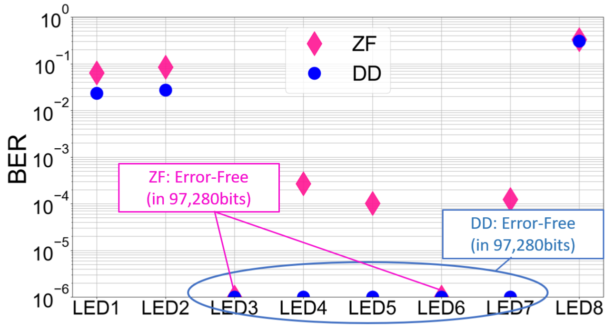

Fig. 6. Bit error rates of each optical modulator at 90 m

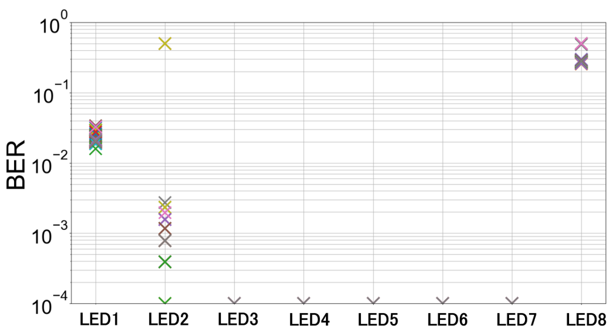

Fig. 7. Frame-wise error rate of each optical modulator at 90 m (Frame 1 to 37)

measure. Upon implementing this scheme, the data to be transmitted is first encoded by an LDPC coder being sent to the transmitter. As shown in Fig. 8, binary temporary received words, generated by signal processing, are decoded based on the reliability of each subchannel; i.e., the BER of each subchannel determined by a training sequence sent prior to data transmission.

C. Simulation Method

To search for an efficient code, we conducted simulations following these steps.

a) Generation of parity-check matrix: A parity-check matrix was generated using Gallagher's construction method [8], corresponding to a code length N, row weight w_r, and column weight w_c.

b) Generation of LDPC codewords: First, a random binary information symbol sequence of length N was generated. The LDPC codeword was then generated using the parity-check matrix created in (a).

c) Generation of the sample received word: To emulate the actual OWC channel, the received word was generated by randomly flipping each symbol of the codeword generated in (b) based on the error rate of each subchannel.

d) Estimation of transmitted word from received word: The transmitted word was estimated from the received word created in (c) using the sum-product algorithm based on the parity-check matrix and BER of each subchannel.

TABLE V
PROBABILITY OF RECEIVING AN INCORRECT 0 OR 1 FOR EACH OPTICAL MODULATOR AT 90M

	LED 1	LED 2	LED 3 to 7	LED 8
P_{e+}	2.99×10^{-3}	3.40×10^{-3}	0	3.94×10^{-2}
P_{e-}	2.89×10^{-3}	3.44×10^{-3}	0	3.68×10^{-2}

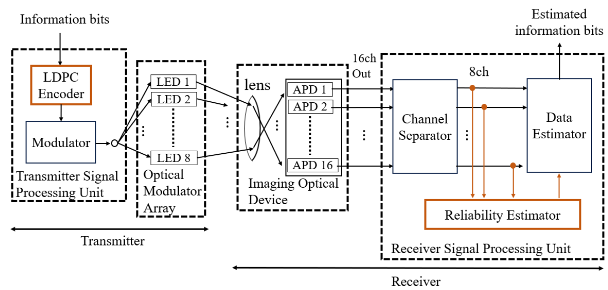

Fig. 8. Proposed system using the pre-measured error rates for each subchannel

e) Calculation of BER: The steps (b)-(d) were repeated 1000 times and the BER was then calculated.

The steps (a)-(e) were repeated 100 times and, the lowest BER of these was recorded.

D. Numerical Results

Table VI shows the parameters of the code with the best at each coding rate. Fig. 9 shows the BER performance against the number of iterations according to individual subchannel BERs of each subchannel at 90 m, as depicted in Fig. 6. The figure indicates the significant improvement in system performance due to LDPC coding. Without coding, the average BER of the eight subchannels is 4.42×10^{-2}, compared to an error-free results with a $R = 0.6$ code. In contrast, when the same reliability value is assumed for all subchannels, the performance was worse than the one when each signal is weighted by the reliability of each subchannel.

To assess the efficiency of coding, we calculated the channel capacities both before and after coding. The channel capacity with and without, C_0 and C_c, respectively are defined by

$$C_0 = \sum_{m=1}^{8} \{1 - h(p_m)\} \tag{2}$$

$$C_c = 8R\{1 - h(p)\} \tag{3}$$

$$h(P) = -P\log_2 P - (1-P)\log_2(1-P) \tag{4}$$

where p_m is the error rate of the m-th subchannel before coding, p is the error rate after coding and R is the coding rate. In an ideal coding scenario, the channel capacity theoretically remains the same before and after coding. Based on this, by solving $C_c = C_0$(Constant Value) for p, the achievable BER (Shannon limit) at any coding rate can be written as a function of the coding rate R. In our study, we numerically calculated this value. Fig. 10 illustrates the BER of the best-performing code for each coding rate, along with the Shannon limit at each coding rate. In our simulation, we found that a code

TABLE VI
PARAMETERS OF CODES

R	N	w_r	w_r	distance	BER
1	No coding			70m	3.63×10^{-3}
				80m	8.36×10^{-5}
				90m	4.42×10^{-2}
0.5	1152	6	3	70m	0
				80m	0
				90m	0
0.6	1040	5	2	70m	0
				80m	0
				90m	0
0.7	2560	10	3	70m	0
				80m	0
				90m	0
0.75	5124	12	3	90m	0
0.8	10230	15	3	70m	0
				80m	0
				90m	1.23×10^{-3}
0.9	10260	30	3	70m	0
				80m	0
				90m	4.27×10^{-2}
0.95	10240	80	4	70m	1.52×10^{-3}
				80m	0

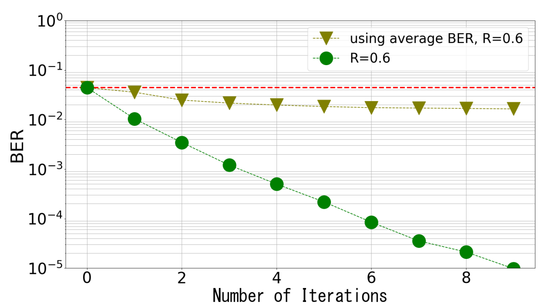

Fig. 9. Comparison of bit error rates at each iteration in decoding (at 90m)

with rates up to 0.75 achieves error-free performance, despite a BER of 4.42×10^{-2} without coding. Furthermore, error-free is achieved with a high coding rate of R = 0.9 at a distance of 70 m, where the BER was 3.63×10^{-3} without coding, and R = 0.95 at a distance of 80 m, where the BER was 8.36×10^{-5}. Even under the challenging condition of a 90m distance, we achieved coding close to the Shannon limit at a coding rate of 0.8 or higher. These results indicate that accounting for performance variations across signal beams, —an issue common optical MIMO systems— through coding and decoding is effective.

V. Conclusion

In this paper, an LED-based optical imaging MIMO system capable of ensuring long-distance transmission at a high date rate is presented. We achieved error-free outdoor transmission of a 200 Mbps data rate over a distance of 100 m. However, the experimental tests also showed that transmission errors occurred at distances shorter than 100 m, leading to a large difference between the BER corresponding to each transmitting LED signal. Therefore, we proposed to apply LDPC coding along with a decoding method that takes into

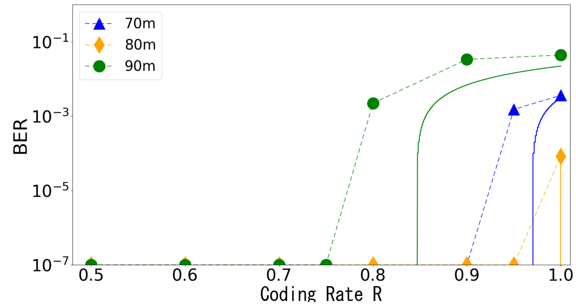

Fig. 10. BER performance of each coding rate

account the BER of each signal beam. Based on our results, an improvement in BER performance can be obtained while considering appropriate code lengths and coding rates at a given distance.

Acknowledgment

The authors would like to thank Prof. Takaya YAMAZATO and Shan LU of Nagoya University for their guidance and encouragement in carrying out this research. A part of this work is based on the Joint Research with Chubu Electric Power Company and IMaSS of Nagoya University.

References

[1] P. W. Berenguer, D. Schulz, J. Hilt, P. Hellwig, G. Kleinpeter, and J. K. Fischer, "Optical wireless MIMO experiments in an industrial environment," IEEE J. Sel. Areas, vol.36, no.1, pp.185-193, Jan. 2018.
[2] D. Takase and T. Ohtsuki, "Optical wireless MIMO communications (OMIMO)," IEEE Global Telecommunications Conference (GLOBECOM), Nov. 2004.
[3] T. Nakamura, C. Ben Naila, K. Kobayashi, H. Okada, and M. Katayama "Experimental evaluation of indoor optical wireless MIMO systems with square and linear array constellations," IEEE Photonnics J., vol.13, no.1, Art., Feb. 2021.
[4] A. K. Gupta and A. Chockalingam, "Performance of MIMO modulation schemes with imaging receivers in visible light communication," IEEE J. Lightwave Technology, vol.36, no.10, pp.1912-1927, Jan.23 2018.
[5] A. Iwasa, C. Ben Naila, K. Kobayashi, H. Okada, and M. Katayama, "Experimental evaluation of an indoor long distance high speed imaging MIMO system," IEEE Global Communications Conference (GLOBECOM), Dec. 2020.
[6] C. Ben Naila, H. Okada, and M. Katayama, " Indoor long distance high speed imaging MIMO system with linear transmitting element array, " IEICE Technical Report, vol.120, no.5, pp.171-175, Mar. 2021.
[7] C. Ben Naila, T. Nakamura, H. Okada, and M. Katayama,"Evaluation of conventional and imaging MIMO OWC systems using linear array design," IEEE Photonics J., vol.14, no.1, Oct. 2022.
[8] R. Gallager, "Low-density parity-check codes," IRE Transactions on Information Theory, vol.8, no.1, pp.21-28, Jan. 1962.
[9] I. B. Djordjevic, S. Denic, J. Anguita, B. Vasic and M. A. Neifeld, "LDPC-Coded MIMO Optical Communication Over the Atmospheric Turbulence Channel," IEEE Global Communications Conference (GLOBECOM), pp. 2220-2225, Nov. 2007.
[10] M. A. Fernandes, P. P. Monteiro and F. P. Guiomar, "400G MIMO-FSO Transmission with Enhanced Reliability Enabled by Joint LDPC Coding," 2021 European Conference on Optical Communication (ECOC), pp. 1-4, Sep. 2021.